

Difference in Surface Properties between Insoluble Monolayer and Adsorbed Film from Kinetics of Water Evaporation and BAM Image

Yoshikiyo Moroi,^{*,†} Muhammad Rusdi,[†] and Izumi Kubo[‡]

Chemistry and Physics of Condensed Matter, Graduate School of Sciences, Kyushu University-Ropponmatsu, Fukuoka 810-8560, Japan, and Faculty of Engineering, Soka University, Tokyo 192-8577, Japan

Received: May 19, 2003; In Final Form: March 1, 2004

The evaporation rate of water molecules across three kinds of interfaces (air/water interface (1), air/surfactant solution interface (2), and air/water interface covered by insoluble monolayer (3)) was examined using a remodeled thermogravimetric balance. There was no difference in both the evaporation rate and the activation energy for the first two interfaces for three types of surfactant solutions below and above the critical micelle concentration (cmc). This means that the molecular surface area from the Gibbs surface excess has nothing to do with the evaporation rate. In the third case, the insoluble monolayer of 1-heptadecanol decreased the evaporation rate and increased the activation energy, indicating a clear difference between an insoluble monolayer and an adsorbed film of soluble surfactant. This difference was substantiated by BAM images, too. The images of three surfactant solution interfaces were similar to that of just the water surface, while distinct structures of molecular assemblies were observed for the insoluble monolayer. The concentration profile of water molecules in an air/liquid interfacial region was derived by Fix's second law. The profile indicates that a definite layer just beneath the air/liquid interface of the surfactant solution is made mostly of water molecules and that the layer thickness is a few times the root-mean-square displacement $\sqrt{2Dt}$ of the water molecules. The thickness was found to be more than a few nanometers, as estimated from several relaxation times derived from the other kinetics than evaporation of amphiphilic molecules in aqueous systems and a maximum evaporation rate of purified water.

Introduction

Surface tension of an intensive thermodynamic variable is not a surface property in a strict sense but a macroproperty including several molecular layers in the bulk, the interface layer above them, and the gaseous phase.

The insoluble monolayer at the air/water interface can decrease the surface tension (γ_0 , 72.0 mN m⁻¹ at 298.2 K) of water down, resulting in the surface tension (γ) or surface pressure ($\pi = \gamma_0 - \gamma$) by collaboration between the insoluble monolayer and the water layers beneath the monolayer. The surface pressure gradually changes with the molecular surface area at the interface, except for a solid condensed film whose surface pressure increases rapidly up to a collapse pressure with little change in the molecular surface area. As for an adsorbed film of soluble amphiphiles or surfactants, the Gibbs surface excess has always been employed to evaluate the molecular surface area at the air/solution interface, which is derived from the change of surface tension against concentration of the soluble surfactant. The Gibbs adsorption isotherm has presented that the molecular surface area obtained is almost constant at concentrations above half critical micelle concentration (cmc) of soluble amphiphiles.^{1,2} This is a big difference in characteristics between an insoluble monolayer and an adsorbed film. Indeed, it has been attempted to measure experimentally the surface excess of soluble amphiphiles,^{3–5} but defining the location of the adsorbed film could not be made definitely clear.

On the other hand, measuring the surface adsorption by neutron scattering is standardized by the Gibbs surface excess.⁶

The above observations strongly indicate that an adsorbed film is quite different from an insoluble monolayer and that the adsorbed film cannot be localized at the air/solution interface. If the surface excess is located at the interface, the interfacial tension should be much less than that at the cmc, on the basis of the fact that the interfacial tension of a double layer film is 0.2–6 m Nm⁻¹, where either side of the interface is in contact with the aqueous bulk.⁷ This observation can be further substantiated by the following fact, too. A black film of soap bubble is made of a double layer of soap molecules, where both sides of the film are in contact with the gaseous phase. Such a film could be made to last as long as 95 days by Dewar in 1917,⁸ which made the pressure difference between inside and outside of the black film almost zero. In other words, surface tension of the film is also very close to zero according to the equation for the Laplace pressure. Judging from the above observations, it seems quite fallacious to reach the conventional conclusion that the surface excess is concentrated at the air/solution interface.

On the other hand, if the interface is covered by an adsorbed film or by an insoluble monolayer, the water evaporation rate should be retarded, and the activation energy for the evaporation should be different from that of water itself. In fact, the evaporation rate and the activation energy across an insoluble monolayer are different from that of water. This article is aimed to clarify the difference between the insoluble monolayer and the adsorbed film by measuring the water evaporation rate, the activation energy, and the Brewster angle microscopy (BAM)

* Corresponding author. Phone: +81-92-726-4742. Fax: +81-92-726-4842. E-mail: moroisc@mbbox.nc.kyushu-u.ac.jp.

[†] Kyushu University-Ropponmatsu.

[‡] Soka University.

image, which enables us to observe the monolayer at the air/solution interface.⁹

The activation energy for water evaporation is quite useful to quantify the process through which evaporation takes place. This can be investigated by determining the temperature dependence on the evaporation rates. The soluble surfactants examined were cationic, anionic, and nonionic to see if there exists any molecular influence on the rate among different types of surfactants. The rate was also examined from the viewpoint of molecular surface area of the amphiphiles at the air/solution interface derived from the Gibbs' adsorption isotherm.¹⁰ The effect of an insoluble monolayer on the water evaporation was also examined using 1-heptadecanol as an insoluble amphiphile.¹¹ Indeed, these results are pertinent to the issue of where the surface excess material is concentrated and to developing a reasonable model for the surface excess of a surfactant solution. Retardation of water evaporation due to the concentration of the surfactant molecules at the air/solution interface could be explained by a change in the activation energy for the evaporation. At the same time, the evaporation rate should present useful information on the gas/liquid interface, because the evaporation takes place just from the interface. From the viewpoint of dynamic surface tension studies, which considers a mechanism for the adsorption process, there is some uncertainty in the transport of surfactant molecule from a subinterface to an interface.^{10,12–14} The present experimental results will endeavor to throw new insight on amphiphile adsorption at the air/solution interface.

Experimental Section

1. Materials. Two surfactant groups were used in this research: water soluble surfactants and an insoluble surfactant. The soluble surfactants were *N*-(1,1-dihydroperfluoro octyl)-*N,N,N*-trimethylammonium chloride (C8-TAC), sodium dodecyl sulfate (SDS), and *N*-decanoyl-*N*-methylglucamide (MEGA-10), cationic, anionic, and nonionic surfactants, respectively. The insoluble surfactant was 1-heptadecanol (C17-OH). The C8-TAC was synthesized in our group,¹⁵ and its purity was more than 99% from NMR analysis. SDS was purchased from Nacalai Tesque and recrystallized several times from water after ether extraction from the dry sample. The purity was checked by elemental analysis. The observed and calculated results (in parentheses) were in satisfactory agreement in weight percentage: C 8.74 (8.78%) and H 49.9 (49.7%). MEGA-10 was purchased from Fluka and used without further purification. The purity indicated was more than 98%. C17-OH was obtained from Tokyo Kasei Kogyo, and the purity was confirmed by surface pressure–molecular surface area curve. All of the soluble surfactants formed an adsorbed film at the air/solution interface just below the cmc:^{15–17} 13.6 mmol dm⁻³ for C8-TAC, 8.2 mmol dm⁻³ for SDS, and 6.5 mmol dm⁻³ for MEGA-10 at 298.2 K. The solutions were examined at two initial concentrations: a half and just below the cmc. The 1-heptadecanol formed an insoluble monolayer, a solid condensed film (a collapse pressure (π^c) = 45 mN m⁻¹ and the molecular surface area (A^c) = 0.20 nm²) at the air/water interface, which was confirmed by the pressure–area curve from the hexane solution at 303.2 K. The water used was distilled twice from alkali permanganate solution.

2. Method. The apparatus was modified from the usual thermogravimetric balance (Rigaku Thermo Plus 2), where the sample pan had a large area of 0.739 cm² to reduce the edge effects as much as possible. A constant volume (150 μ L) of liquid sample was pipetted into a shallow platinum pan for the

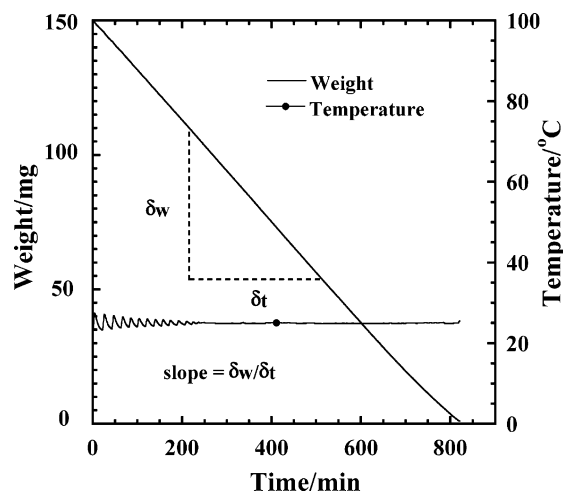


Figure 1. Typical change of weight with time.

thermogravimetric measurement, where the height from the surface of the liquid to the top of the pan was 0.480 cm. The apparatus monitored the change in weight as a function of the temperature with time. The temperature was controlled within ± 0.1 °C throughout the run except for the initial stabilization period less than 3 h at 25 °C (Figure 1). This stabilization period became shorter with increasing temperature, less than 30 min at 60 °C. The moisture in the air was completely removed by passing it through concentrated sulfuric acid and then by storing it over dried silica gel. Then, the dry air was passed twice through a filter of pore size 0.22 μ m (Millipore, SLGV025LS) to remove dust, and the flow rate was controlled by a flow meter with a needle bulb.¹⁸ The experimental reproducibility was such that the weight loss with time could trace a line for the same sample.

The run was started without allowing for thermal equilibrium with the furnace temperature because of the small thermal mass of the sample. For the 1-heptadecanol sample, purified water with a tiny solid particle placed on the surface was kept in 100% relative humidity for 1 day in the pan. This procedure was to allow the spreading monolayer to be in equilibrium with the solid phase prior to starting the run.

A Brewster angle microscope (Nippon Laser Electronics Laboratory, NL-EMM633) was placed above the surfactant solutions whose concentration was just below cmc or above the insoluble monolayer under equilibrium spreading pressure. Initially, the angle of illumination was adjusted to the Brewster angle to minimize the reflected light from the water surface. The dark image means that most of the light illuminated onto the water surface does not reflect from the surface. If there was a condensed layer of amphiphiles, more light was reflected from the surface and bright images could be observed. Images were taken with a CCD camera and recorded on a videotape by using a video system (video recorder, video monitor, and video printer). The recorded BAM images were transferred to a computer using analysis software and processed. These procedures were made at room temperature.

Results and Discussion

Generally, most surface scientists drew a model for the surface excess of a surfactant solution as shown in Figure 2a. In the figure, the surfactant molecules are supposed to accumulate at the surface of the solution. It looks similar to a model for the insoluble monolayer at the air/water interface (Figure 2b). Numerous articles and fundamental books have been published on the insoluble monolayer and on the adsorbed film which

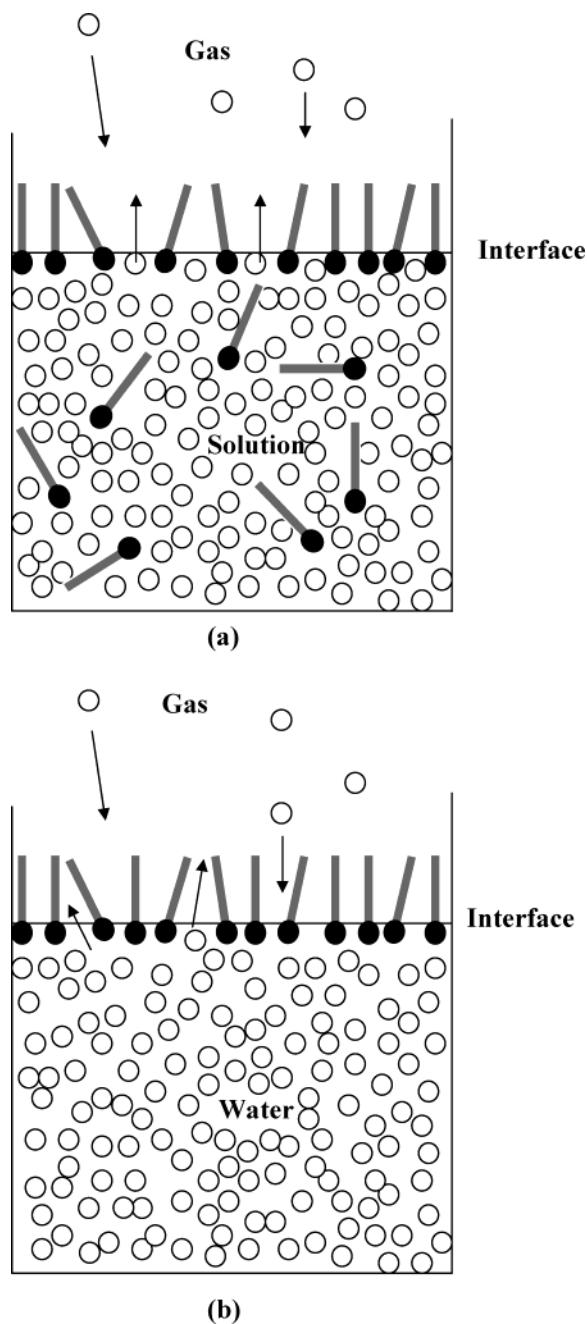


Figure 2. Conventional model of surfactant solution (a) and insoluble monolayer model (b).

are discussed in terms of the Gibbs adsorption isotherm.^{5,19–22} For the insoluble monolayer, a molecular surface area can be clearly defined, because all of the molecules added on a surface are located exclusively at the air/liquid interface. However, the molecular surface area is derived from the surface excess that is calculated from the Gibbs adsorption isotherm, which is obtained from the plot of surface tension vs concentration. Sometimes, the molecular surface area obtained can occupy more than 80% of the air/solution interface, even when the molecules stand vertically against the interface.¹⁵ It is certain that the Gibbs adsorption isotherm leads to an excess amount of amphiphiles, and therefore, the molecular surface area obtained has nothing to do with a real molecular surface area at the air/solution interface. If this is correct, it is meaningless to calculate the molecular surface area of the adsorbed film as depicted in Figure 2a. However, every textbook says that a decrease in interfacial tension is due to concentration of surface-

active agents at the air/solution interface. If the above statement is correct, there would be an expected difference in the evaporation rate or activation energy for water evaporation between that from purified water and that from an aqueous surfactant solution. In reality, however, there is no difference between them. In addition, if the model depicted in Figure 2a is correct, the surface tension should be less than a few millinewton per meter, as mentioned in the Introduction section.

The evaporation rates of purified water over the temperature range 298.2–333.2 K were measured to obtain the activation energy for evaporation.²³ In the present study, these data were used as a reference point to clarify the effect of the soluble surfactants in solution on the evaporation rate and to differentiate between aqueous surfactant solutions and water covered by an insoluble monolayer. The evaporation rate in units of $\text{mol s}^{-1} \text{cm}^{-2}$ was calculated from the slope after the initial drift period (Figure 1). The activation energy of water evaporation from surfactant solution and from bulk water covered by insoluble monolayer can be calculated from the temperature dependence of the evaporation rate employing the Arrhenius equation

$$\ln k = \ln A - \frac{E_a}{RT} \quad (1)$$

where k is evaporation rate per unit area ($\text{mol s}^{-1} \text{cm}^{-2}$), A is an arbitrary constant, E_a is the activation energy (J mol^{-1}). Thus, E_a can be obtained by analyzing the evaporation rates according to eq 1. This definition applies regardless of whether the Arrhenius plot is linear or not. If it is not, the activation energy changes with temperature.

1. Soluble Surfactant Solution. The evaporation rate of water across the air/surfactant solution interface was measured, and the results are given in Table 1. According to the data, the evaporation rates of water from purified water and the surfactant solutions (anionic, cationic, and nonionic) are the same within experimental error of $\pm 2.5\%$ over the temperature range of 298.2–328.2 K at the two initial concentrations, half and just below the cmc. This means that the activation energies for water evaporation from the surfactant solutions are the same as that from purified water. This important result suggests that there is no additional barrier for water evaporation caused by concentration of surfactant molecules or excess amount of surfactant molecules at the air/solution interface. The molecular surface areas from the Gibbs surface excess were evaluated by the surface tension vs concentration relationship, which are also listed in Table 1. The results indicate that at the air/solution interface the surfactant molecules are fairly close-packed just below the CMC. Nevertheless, there was no retardation for water evaporation from the soluble surfactant solutions. The C17–OH monolayer with the molecular surface area of ca. 0.22 nm^2 at $\pi < 15 \text{ mN m}^{-1}$ showed significant influence on the evaporation rate. These results give rise to the following questions: Why does the surface excess not reduce the water evaporation rate and where are the surfactant molecules concentrated? These points will be discussed later.

2. Insoluble Monolayer. Further experiments on the insoluble monolayer at an equilibrium spreading pressure were carried out to further understand the effect of its presence at the air/water interface on the evaporation rate of water. Representative plots of weight decrease of water from purified water, soluble surfactant solutions, and water covered by insoluble monolayer (C17–OH at 38 mN m^{-1}) are plotted in Figure 3. From Figure 3, the weight decrease of water covered by C17–OH monolayer is significantly slower than those of just liquid water and the soluble surfactant solutions, whereas the difference between just

TABLE 1: Evaporation Rate of Water Across Air–Surfactant Solution Interface

system	initial concentration	$\gamma^a/\text{mN m}^{-1}$	MSA ^b /nm ²	evaporation rate/ mg min ⁻¹			
				298.2 K	308.2 K	318.2 K	328.2 K
SDS/H ₂ O	0.5 cmc	52.4	0.41	0.254	0.467	0.801	—
	1.0 cmc	40.0		0.250	0.468	0.817	—
C8-TAC/H ₂ O	0.5 cmc	32.4	0.40	0.250	0.447	0.814	—
	1.0 cmc	20.0		0.247	0.468	0.802	—
MEGA-10/H ₂ O	0.5 cmc	35.9	0.34	—	0.459	0.810	1.331
	1.0 cmc	30.3		—	0.455	0.793	1.342
H ₂ O	—	—	—	0.260	0.455	0.810	1.357

^a Surface tension at 298.2 K. ^b Molecular surface area at 298.2 K.

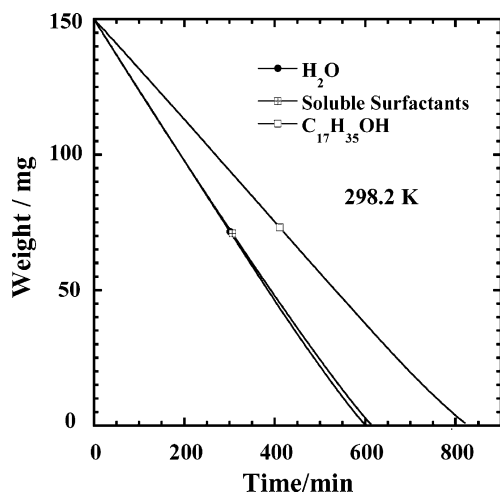


Figure 3. Evaporation rate of water across air/liquid interfaces.

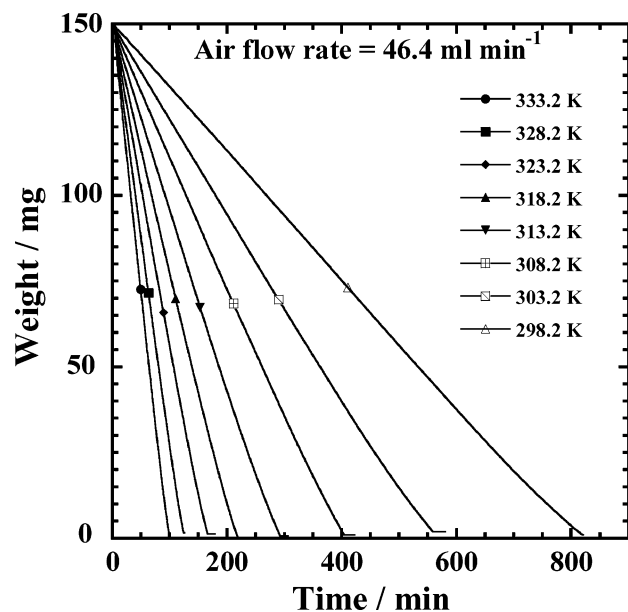


Figure 4. Evaporation rate of water across air/water interface covered by insoluble monolayer of C17–OH.

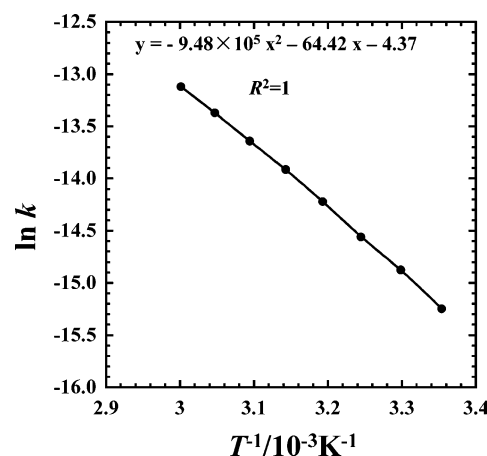
liquid water and aqueous solution of the soluble surfactants is within the experimental error as mentioned above. The slight retardation of weight decrease after 70% evaporation of the total weight for soluble surfactant solutions is due to change in concentration of the surfactant molecules in the solution.

Figure 4 shows the weight decrease of water covered by C17–OH monolayer over the temperature range of 298.2–333.2 K. This result clearly indicates the slower evaporation rate for water molecules passing across the insoluble monolayer, which acts as a resistance for flux of water molecules.²⁴ A constant rate of weight loss was observed up to 80% of the total weight,

TABLE 2: Evaporation Rate (ER) of Water Covered by Insoluble Monolayer

T/K	ER/mg min ⁻¹	k/mol s ⁻¹ cm ⁻²	ln k (y) ^a	activation energy	
				C ₁₇ H ₃₅ OH	water ^b
298.2	0.1909	2.39×10^{-7}	-15.2	53.4	48.0
303.2	0.2771	3.47×10^{-7}	-14.9	52.5	47.4
308.2	0.3802	4.76×10^{-7}	-14.6	51.7	46.8
313.2	0.5326	6.67×10^{-7}	-14.2	50.9	46.2
318.2	0.7241	9.07×10^{-7}	-13.9	50.1	45.6
323.2	0.9472	1.19×10^{-6}	-13.6	49.3	45.1
328.2	1.2473	1.56×10^{-6}	-13.4	48.6	44.6
333.2	1.6063	2.01×10^{-6}	-13.1	47.9	44.1

^a y is the ordinate value in Figure 5. ^b Data from ref 23.

Figure 5. Plots of $\ln k$ vs T^{-1} for water covered by insoluble monolayer: $y = \ln k$ and $x = T^{-1}$.

above which the sample pan was not uniformly covered by liquid.

The activation energy of water evaporation across the insoluble monolayer can be obtained by the same method as previously described. The parameters needed are listed in Table 2 and plotted in Figure 5. Because the slope of $\ln k$ vs T^{-1} plot is not linear, the activation energy of the evaporation changes with temperature. The values are given in column 5 of Table 2. According to the values, the activation energy of water evaporation across the monolayer is higher than that from the surface of liquid water and surfactant solutions (Figure 6). This is caused by the molecular resistance of the C17–OH monolayer to evaporation, where the monolayer is a solid condensed state judging from the equilibrium spreading pressure.²⁵ Now, it is quite evident that the insoluble monolayer of 1-heptadecanol can reduce the water evaporation rate and increase the activation energy.

The decrease in activation energy with increasing temperature (Figure 6) can be interpreted by less energy needed for the water molecules to evaporate at higher temperatures. This is because the π –A curve shifts to a larger molecular area with increasing

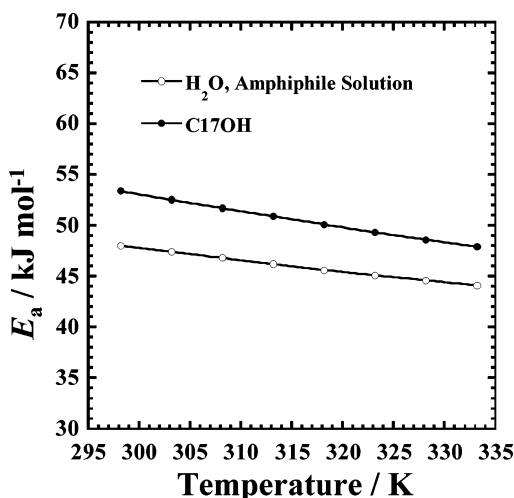


Figure 6. Dependence of the activation energy of water evaporation on temperature for purified water, amphiphile solutions, and water covered by insoluble monolayer of C17–OH.

temperature.²⁶ The lack of break point on the curve in Figure 6 indicates that the spreading monolayer is stable as a condensed solid state over the experimental temperature range examined.

3. BAM Images of Surfaces. Dark BAM images of surfaces for just water and three surfactant solutions at the cmc are illustrated in Figure 7a, where nothing is observed on the surfaces. In addition, there is no difference among the three solution samples in darkness, either. This fact strongly suggests no condensation of soluble surfactants at the surface. However, for the MEGA-10 solution only, when it was left for 1 h or more under aerobic atmosphere, some structures were observed on small parts of the surface (Figure 7b). This will be discussed later.

The C17–OH monolayer was spread from either a chloroform solution or the solid placed on water surface. For the latter case, the BAM image was taken 1 day later, which means that the monolayer is under an equilibrium spreading pressure ($\pi^{\text{eq}} = 39 \text{ mN m}^{-1}$ and the molecular area $= 0.20 \text{ nm}^2$ at 298.2 K; these are very close to reference values²⁷). The images of C17–OH monolayer spread by both methods were quite similar (Figure 7c). The bright images and their structure indicate the organized assembly of islands of C17–OH molecules at the surface, which are quite different from those for the surfactant solutions. The structure indicates that the molecules are not homogeneously dispersed at the surface.

The BAM images were taken twice for each sample using different sample solutions to ascertain their reproducibility. The above difference in surface structure between the surfactant solutions and the insoluble monolayer can substantiate the difference in water evaporation between them.

4. Appropriate Model of Surfactant Solution. The number of surfactant molecules, which are able to go up to an interfacial region, should increase with increasing surfactant concentration below the cmc according to the Gibbs adsorption isotherm. In other words, a molecular surface area is supposed to decrease with increasing surfactant concentration below or near the cmc. If, therefore, surfactant molecules are able to really go up to the surface, a reduction of water evaporation rate should be observed. In reality, however, there is no reduction of the evaporation rate. We can assume therefore that they locate at some distance below the surface, which makes enough space for water molecules to escape freely to the gas phase, as is the case for just bulk water. That is, the water layer just beneath an air/surfactant solution interface should be deeper than a definite

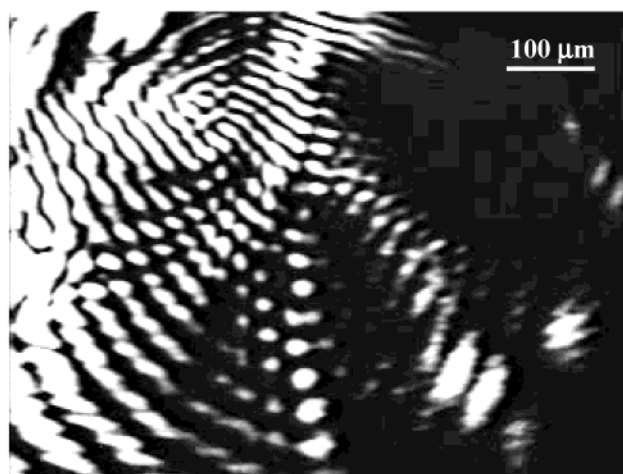
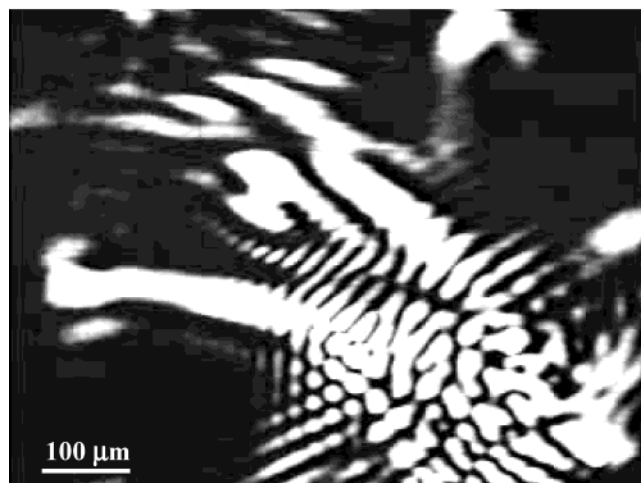
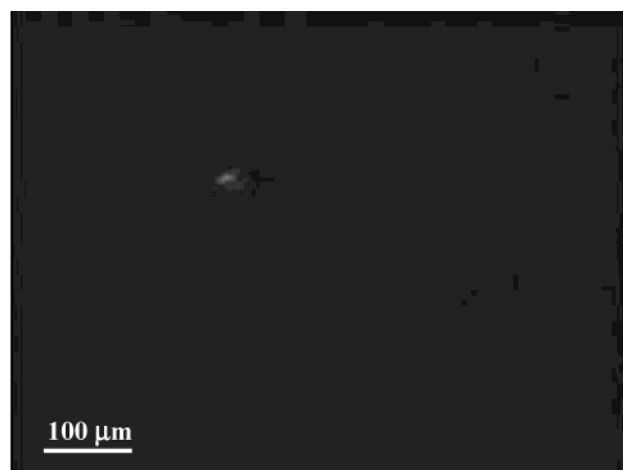


Figure 7. (a) BAM images for just water and surfactant solutions of C8-TAC, SDS, and MEGA-10 at the cmc, (b) BAM image of some parts of MEGA-10 solution, and (c) BAM image of insoluble monolayer of C17–OH.

depth so that the water evaporation rate from the solution may be identical with that of liquid water itself. At the same time, soluble surfactant molecules must move downward to the inner aqueous bulk so that the upper water layer may keep this finite depth. Otherwise, the surfactant molecules would concentrate in the layer, leading to slower evaporation rate of water or higher activation energy of vaporization. Indeed, the amount of surface excess was examined using a radioactive surfactant, and the amount was found to be equal to that expected from the Gibbs'

adsorption isotherm.^{3,4} Unfortunately, however, the location of excess amount was not manifested at all in the articles.

Now, the surfactant molecules are in dynamic equilibrium between interfacial region and bulk phase. Their exchange in position between them should change the structures of water molecules in the interfacial region from one of more hydrogen bonding to less hydrogen bonding among them. This should make the activation energy decrease, even if the evaporation rate becomes slower than that of just water. On the contrary, both the evaporation rate and the activation energy from the surfactant solutions are the same as pure water. The rate of movement of surfactant molecules can be compared with an escape rate of amphiphiles from their parent micelles or with an escape rate of solubilize molecules from their parent aggregates. The former rate constant is of the order 10^5 s^{-1} for SDS,²⁸ while the latter is of the order 10^6 to 10^7 s^{-1} .²⁹ The relaxation time then becomes 10^{-5} to 10^{-7} s^{-1} . The root-mean-square displacement (\bar{x} , rms) of water molecules during this period of time (t) can be estimated from the diffusion coefficient D by the equation $\bar{x} = \sqrt{2Dt}$.

Using this relationship, we found that the depth of the water layer becomes roughly 21.0–210 nm, when the self-diffusion coefficient of water ($2.28 \times 10^{-5} \text{ cm}^2 \text{ s}^{-1}$) was used.³⁰ In this sense, the water evaporation from the surfactant solution can be inferred to be taking place under the condition that a concentration profile of surfactant molecules is very close to that in adsorption equilibrium. This is also expected for a long period of time (2 h at least) taken for evaporation of only a 150 μL sample liquid (see Figure 4).

To ascertain the validity of the presumption above, the following theoretical calculation was made for water transport across the air/water interface by diffusion. Fick's differential equation for water phase and for gaseous phase is given by equations 2 and 3, respectively:³¹

$$\frac{\partial c}{\partial t} = D^I \frac{\partial^2 c}{\partial x^2} \text{ for liquid phase } (x < 0) \quad (2)$$

$$\frac{\partial c}{\partial t} = D^{II} \frac{\partial^2 c}{\partial x^2} \text{ for gas phase } (x > 0) \quad (3)$$

where D^I and D^{II} are the diffusion coefficients for a liquid phase and a gaseous phase, respectively.

The initial conditions are $c = c_0$ for $x < 0$ and $c = 0$ for $x > 0$ at $t = 0$.

Continuity of flow must satisfy the following equation:

$$D^I \left(\frac{\partial c}{\partial x} \right)_{x=0}^I = D^{II} \left(\frac{\partial c}{\partial x} \right)_{x=0}^{II} \quad (4)$$

The solutions for the above are

$$c = c_0 \left\{ 1 - \frac{\kappa \sqrt{D^{II}}}{\kappa \sqrt{D^{II}} + \sqrt{D^I}} \left[1 + \operatorname{erf} \left(\frac{x}{2\sqrt{D^I t}} \right) \right] \right\} \text{ for } x < 0 \quad (5)$$

$$c = c_0 \frac{\kappa \sqrt{D^I}}{\kappa \sqrt{D^{II}} + \sqrt{D^I}} \left[1 - \operatorname{erf} \left(\frac{x}{2\sqrt{D^{II} t}} \right) \right] \text{ for } x > 0 \quad (6)$$

where

$$\frac{(c^{II})_{x=0}}{(c^I)_{x=0}} = \kappa$$

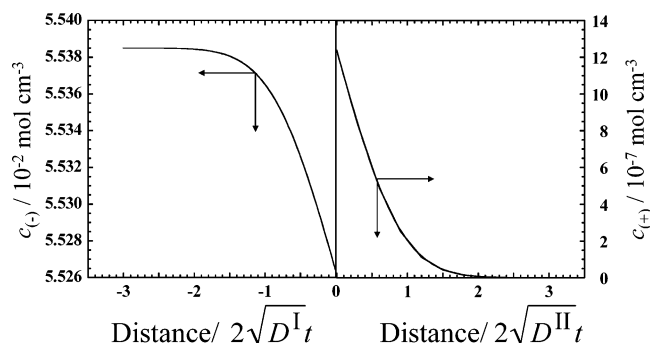


Figure 8. Concentration profile of water molecule in the interfacial region. $D^I = 2.28 \times 10^{-5} \text{ cm}^2 \text{ s}^{-1}$, $D^{II} = 2.19 \times 10^{-1} \text{ cm}^2 \text{ s}^{-1}$.

Flux at interface:

$$J = -D^{II} \left(\frac{\partial c}{\partial x} \right)_{x=0}^{II} = \frac{c_0 \kappa \sqrt{D^I} \sqrt{D^{II}}}{\kappa \sqrt{D^{II}} + \sqrt{D^I}} \times \frac{1}{2\sqrt{t}} \quad (7)$$

The concentration profile of water derived from the above is shown in Figure 8. As can be seen from the figure, the concentration change can be observed within the range of a few rms displacements. If the concentration profile were disturbed by the presence of amphiphiles, the evaporation rate of water would change. In other words, the concentration profile should not be disturbed by amphiphile molecules, which means that they are located below a water layer of a few rms displacements.

We assume the following two concentrations at stationary state: one is $c_0 = 5.538 \times 10^{-2} \text{ mol cm}^{-3}$ for the bulk side and the other is $c_{x=0}^{II} = 1.240 \times 10^{-6} \text{ mol cm}^{-3}$ for the gaseous side. The former is the molar concentration of liquid water at 298.2 K, while the latter is equivalent to a saturated vapor pressure at 298.2 K. The diffusion coefficient D^I is the self-diffusion coefficient of $2.28 \times 10^{-5} \text{ cm}^2 \text{ s}^{-1}$ ³⁰ and D^{II} is the reference data of water vapor of $2.19 \times 10^{-1} \text{ cm}^2 \text{ s}^{-1}$.³² Here, the κ value turned out to be 2.24×10^{-5} from Figure 8. As for the bulk water side (I), the water concentration slightly decreases approaching the interface. At the same time, it is found that the concentration change over twice $2\sqrt{D^{II}t}$ determines the evaporation rate of water according to Fick's law. This is also the case for the gaseous side (II), where the concentration decreases to zero at twice $2\sqrt{D^I t}$. This concentration profile is quite important for the water evaporation across an insoluble monolayer and an adsorbed film. If the amphiphilic molecules in the adsorbed film were concentrated in the region of twice $2\sqrt{D^I t}$, the water evaporation rate should not be equal to that of just liquid water because of destruction of the concentration profile. In other words, the concentration profile of water molecules in the air/liquid interfacial region should be the same for the liquid water and the surfactant solutions. Otherwise, the water evaporation rate becomes different. This means that a finite layer just beneath the air/surfactant solution interface is made of water molecules only, whose depth is more than twice the rms displacement ($\sqrt{2Dt}$) of water molecules. If not, the amphiphile molecules would concentrate in the layer, leading to a slower water evaporation rate or a higher activation energy of the evaporation. It is also highly possible that water molecules move much faster than surfactant molecules and produce the upper layer made of water molecules by rapidly crossing the concentrated surfactant region, which allows the layer of surfactant molecules to locate further beneath the air/solution

interface. Therefore, the concentration profile of the water molecules is determined by the slower diffusion of the surfactant molecules.

Another important result can be derived from the concentration profiles above. From the slope at the boundary, the flux of water molecules (J) across the interface or the evaporation rate of water can be evaluated using the diffusion coefficient ($J = -D\partial c/\partial x$). The evaporation rate at steady state can be experimentally determined, and therefore, the time period to reach the steady state can be obtained from the evaporation rate of purified water using eq 7. The time period of 0.24 ns measured can be compared with the relaxation time above. On the other hand, from the experimental evidence of Bond and Puls for a pure liquid, the surface phase is established, and the static value for the surface tension is reached in less than a nanosecond.³³ This time is, therefore, one estimated limit for the present numerical examination. The depth of the water layer of surfactant solution can, therefore, be calculated by inserting the above values to $x = 2\sqrt{Dt}$, which leads to $x = 3.0$ nm for the unit of abscissa of Figure 8. The value of 6.0 nm is the minimum depth for the water layer, but a more reasonable value would be determined from the surfactant molecules as mentioned above. In fact, an air bubble in cationic surfactant solution is negatively charged, which indicates that the water molecules keep their original structure at the air/solution interface.³⁴

The important conclusions pertaining to the present evaporation rates of water molecules across air/water interface, air/surfactant solution, and air/water covered by an insoluble monolayer can be summarized as follows:

1. There exists no difference in either evaporation rate of water or its activation energy between purified water and three kinds of surfactant solutions below and at the cmc. This means that the molecular surface area from the Gibbs surface excess has no relation with the evaporation rate.
2. The insoluble monolayer decreased the water evaporation rate and increased the activation energy, indicating a clear difference between an insoluble monolayer and a conventional adsorbed film of soluble amphiphiles.
3. The difference in surface between the adsorbed film (item 1) and insoluble monolayer (item 2) was substantiated by the respective BAM images.
4. The concentration profile of water molecules in an air/liquid interfacial region should be the same between liquid water and surfactant solutions. Otherwise, the water evaporation rate becomes different. This means that a finite layer just beneath the air/surfactant solution interface is made of water molecules only, whose depth is longer than twice the rms displacement ($\sqrt{2Dt}$) of the water molecules. If not, amphiphile molecules would concentrate in the layer, leading to slower evaporation rate or higher activation energy of the vaporization.
5. The layer is deeper than a few nanometers, as estimated from several relaxation times for amphiphiles in aqueous systems and from the maximum vaporization rate of purified water.

Finally, if a gas (air) phase in Figure 2a is replaced by an organic liquid, namely at an oil/water interface, soluble amphiphiles can really concentrate at the oil/water interface just as depicted by the figure, because the concentration at the interface is energetically favorable. However, is the molecular concentration at the air/solution interface as depicted in Figure 2a energetically favorable? It is true that the molecular concentration really takes place in the interfacial region, judging from the simple fact that a surface tension increases immediately after cleaning the surface by suction of the interfacial region of

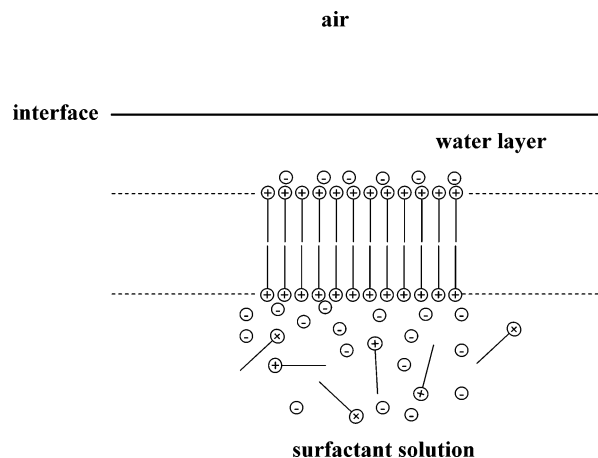


Figure 9. New model of soluble ionic surfactant solution for interfacial region.

surfactant solution through a pipet. Taking the whole matter mentioned above into consideration, the molecular concentration depicted in Figure 9 is much easier to accept from the free-energy point of view.³⁵ In other words, bilamellar layer formation or bilamellar micellization seems quite possible at some distance apart below the interface, where hydrophobic tails contact one another intruding inward from the upper and lower sides by placing headgroups at the surface, just as a structure of a cell membrane. Then, the lamellar surface is positively charged for a cationic amphiphile, while negatively charged for an anionic amphiphile. High charged aggregates cannot come closer to the air/water interface by the repulsive image force, which is also the case for a negative adsorption for ionic salts. Electrostatic force is a long-range force. Thus, water layer with a certain depth is formed between air and the aggregates, which can give rise to the same evaporation rate of water, the same activation energy, and no BAM image just like bulk water. On the contrary, the lamellar surface of nonionic aggregates is electrically neutral. Therefore, no repulsive image force acts onto the lamellar aggregates, and the aggregates can come closer to the air/water interface still keeping some layers of water molecules, which resulted in the appearance of the BAM image. The above bilamellar aggregate formation can explain saturation of the surface excess at ca. half cmc, although surface tension decreases with increasing concentration up to the cmc. That is, after completion of the aggregate formation around half cmc, the concentration of monomeric surfactant keeps increasing above it. On the other hand, the critical concentration for bilamellar aggregate formation can be suggested at very low concentration by a sudden decrease in surface tension vs concentration curve.³⁶ The corresponding sudden increase in the surface excess suggests a commencement of the aggregate formation below the air/water interface.

From the matters above, the surface tension lowering by an insoluble monolayer at the air/water interface is different in essence from the lowering by concentration of amphiphiles below the interface, where the latter lowering really results from the surface excess as expressed by the Gibbs adsorption isotherm. The former lowering is forced to be made in a few molecular layers just around the air/water interface by condensing insoluble molecules to a smaller area by an outside force, while the latter lowering automatically results from condensation of soluble amphiphiles over many molecular layers below the air/water interface.

Acknowledgment. This work was supported by a Grant-in-Aid for Scientific Research No. 10554040 from the Ministry

of Education, Science, and Culture, Japan, and The Cosmetology Research Foundation, which are gratefully acknowledged. We are grateful to Prof. Shinsaku Maruta of Soka University for BAM image processing.

References and Notes

- (1) Gibbs, J. W. *The Collected Works of J. W. Gibbs*; Longmans: New York, 1928.
- (2) Moroi, Y. *Micelles: Theoretical and Applied Aspects*; Plenum Press: New York, 1992; Chapter 8.
- (3) Muramatsu, M.; Tajima, K.; Sasaki, T. *Bull. Chem. Soc. Jpn.* **1968**, *41*, 1279.
- (4) Tajima, K.; Muramatsu, M.; Sasaki, T. *Bull. Chem. Soc. Jpn.* **1970**, *43*, 1991.
- (5) Defay, R.; Prigogine, I.; Bellemans, A.; Everett, D. H. *Surface Tension and Adsorption*; Longmans: London, 1966; Chapter 7, p 92.
- (6) Lu, J. R.; Thomas, R. K.; Penfold, J. *Adv. Colloid Interface Sci.* **2000**, *84*, 143.
- (7) Tien, H. T. *Bilayer Lipid Membrane (BLM): Theory and Practice*; Marcel Dekker: New York, 1974; Chapter 3.
- (8) Dewar, J. J. *Franklin Inst.* **1919**, *188*, 713.
- (9) Kubo, I.; Adachi, S.; Maeda, H.; Seki, A. *Thin Solid Films* **2001**, *393*, 80.
- (10) Eastoe, J.; Dalton, J. S. *Adv. Colloid Interface Sci.* **2000**, *85*, 103.
- (11) *Retardation of Evaporation by Monolayers: Transport Process*; La Mer, V. K., Ed.; Academic Press: New York, 1962.
- (12) Liggieri, L.; Ravera, F.; Passerone, A. *Colloids Surf., A* **1996**, *114*, 351.
- (13) Chang, C. H.; Frances, E. I. *Colloids Surf., A* **1995**, *100*, 1.
- (14) Filippov, L. K. *J. Colloid Interface Sci.* **1994**, *163*, 49.
- (15) Yamabe, T.; Moroi, Y.; Abe, Y.; Takahashi, T. *Langmuir* **2000**, *16*, 9754.
- (16) Mukerjee, P.; Mysels, K. J. *Natl. Stand. Ref. Data Ser. U.S. Natl. Bur. Stand.* **1971**, *36*, 51.
- (17) Okawauchi, M.; Hagio, M.; Ikawa, Y.; Sugihara, G. *Bull. Chem. Soc. Jpn.* **1987**, *60*, 2719.
- (18) Moroi, Y.; Yamabe, T.; Shibata, O.; Abe, Y. *Langmuir* **2000**, *16*, 9697.
- (19) Osipow, L. I. *Surface Chemistry*; Reinhold: New York, 1962.
- (20) Adamson, A. W.; Gast, A. P. *Physical Chemistry of Surfaces*, 6th ed.; Interscience: New York, 1997.
- (21) Bikerman, J. J. *Physical Surfaces*; Academic Press: New York, 1970.
- (22) Hiemenz, P. C. *Principles of Colloid and Surface Chemistry*; Marcel Dekker: New York, 1986.
- (23) Rusdi, M.; Moroi, Y. *Bull. Chem. Soc. Jpn.* **2003**, *76*, 919.
- (24) Archer, R. J.; La Mer, V. K. *J. Phys. Chem.* **1955**, *59*, 200.
- (25) Fukuda, K.; Kato, T.; Machida, S.; Shimizu, Y. *J. Colloid Interface Sci.* **1979**, *68*, 82.
- (26) Harkins, W. D.; Copeland, L. E.; *J. Phys. Chem.* **1942**, *10*, 272.
- (27) Gains JR, G. L. *Insoluble Monolayer at Liquid-Gas Interfaces*; Interscience Publisher: New York, 1966; pp 213–214.
- (28) Moroi, Y. *Micelles: Theoretical and Applied Aspects*; Plenum Press: New York, 1992; Chapter 4.
- (29) Zana, R. *Surfactant Solutions: New Methods of Investigation*; Marcel Dekker: New York and Basel, 1987; Chapter 5.
- (30) Eastal, A. J.; Edge, A. V.; Woolf, L. A. *J. Phys. Chem.* **1984**, *88*, 6060.
- (31) Jost, W. *Diffusion*; Academic Press: New York, 1960; Chapter 1.
- (32) *Handbook of Chemistry and Physics*, 82nd ed.; David, R. L., Ed.; CRC Press: Boca Raton, FL, 2001–2002; pp 6–192.
- (33) Bond, W. N.; Puls, H. O. *Philos. Mag.* **1937**, *24*, 864.
- (34) Murata, T.; Kamio, K.; Sakai, M.; Yamauchi, A. In *Abstracts of the 1994 Joint Meeting of Kyushu-Chugoku-Shikoku Branches in Fukuoka University*; Yomei Press: Fukuoka, 1994; p 250.
- (35) Mukerjee, P. *Micellization, Solubilization, and Microemulsions*; Mittal, K. L., Ed.; Plenum Press: New York, 1977; Vol. 1, p 171.
- (36) Motomura, K.; Iwanaga, S.; Hayami, Y.; Uryu, S.; Matuura, R. *J. Colloid Interface Sci.* **1981**, *80*, 32.